LASER
& PHOTONICS
REVIEWS

Laser Photonics Rev. **8,** No. 6, 896–903 (2014) / **DOI** 10.1002/lpor.201400056

ORIGINAL
PAPER

Abstract The spaser offers an opportunity to achieve coherent optical sources at nanometer scales due to the extreme confinement of optical fields. However, achievement of spasers with directional propagation in the visible wavelength region remains a challenge thus far, owing to the unique optical feedback mechanism and large dissipative losses of the metal cavity. Here, we experimentally demonstrate for the first time a spaser showing highly directional emission in the visible by using a periodic subwavelength hole array perforated in a metal film, which function as plasmonic nanocavities, along with an organic laser dye to supply gain. The lasing occurs in the red wavelength region and shows a single mode. It is suggested that the optical feedback for spasing is provided by the SPP–Bloch wave, which is supported by the fact that no spasing was attained in aperiodic holes as well as in periodic holes that do not support the SPP–Bloch wave at the spasing wavelength.

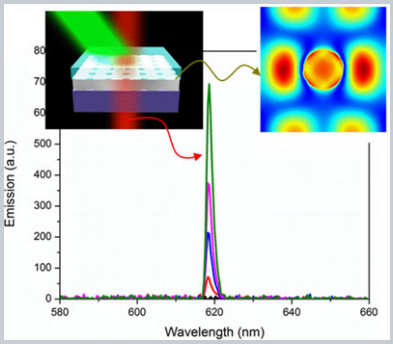

Highly directional spaser array for the red wavelength region

Xiangeng Meng*,, Jingjing Liu**, Alexander V. Kildishev, and Vladimir M. Shalaev***

1. Introduction

The emerging field of plasmonics, dealing with electron–photon interactions at the metal–dielectric interface, is stimulating the search for nanoscopic coherent optical sources [1–13]. Such devices are created through surface plasmon (SP) amplification by stimulated emission of radiation (spaser) [1]. In contrast to conventional lasers, a spaser is not diffraction–limited, and thereby the development of spasers promises revolutionary breakthroughs in nanophotonics. The first spaser with a deep–subwavelength dimension in all three directions was reported in 2009 using a 44 nm core–shell nanostructure with a gold core as the plasmonic nanocavity and a dye–doped silica shell as the optical gain medium [14]. In parallel, a spaser with deep–subwavelength confinement of the optical mode was achieved using a hybrid plasmonic waveguide composed of a CdS nanowire separated from a silver film by a 5 nm–thick MgF_2 dielectric layer [15]. These two proof–of–concept devices have promptly inspired extensive research interests by addressing the amplification of both localized SPs and propagating surface plasmons (also known as surface plasmon polaritons, SPPs) [16–26].

In spite of the increasing number of reports in this exciting area, several challenges still remain. First, spasers in the visible are difficult to attain. The currently demonstrated spasers in the visible mostly operate near $\lambda = 500$ nm [14–21], two of which demonstrated spasing with a resonant wavelength approaching $\lambda = 600$ nm [20, 21]. The second challenge is room–temperature operation for spasers. This challenge arises especially when using semiconductors as the gain media, because their high non–radiative recombination rate at room temperature significantly reduces the optical gain (traditionally not a limitation for organic dyes) [14]. The third, but yet equally important challenge, is the control of the emission direction of spasers. These challenges originate primarily from the high ohmic losses inherent in metals and their effect on the optical feedback mechanism required for lasing. A recent numerical study suggests that breaking the geometric symmetry of a plasmonic core–shell nanocavity serves as an effective route to achieve unidirectional spaser emission [12].

Recently, an approach based on the use of plasmonic crystals to achieve spasers has been proposed [27–31]. The principle is to utilize gap states formed among subwavelength apertures perforated in a metal film or among a metal nanoparticle array to supply sufficient optical feedback for spasing. It was theoretically predicated that a narrow beam of coherent light can be produced due to continuous–wave superradiance in a system composed of a metal film perforated with a periodic hole array as plasmonic nanocavities [27, 28]. Spasing in plasmonic crystals has been experimentally demonstrated as well recently by using either a metal hole array or a metal nanoparticle array to provide optical feedback [29, 30], but these spasers operate in the near–infrared (NIR) wavelength region and the counterpart in the visible has not been experimentally reported so far.

School of Electrical & Computer Engineering and Birck Nanotechnology Center, Purdue University, 1205 West State Street, West Lafayette, IN 47907-2057, USA
**These authors contributed equally to this work.
*Corresponding author(s): e-mail: mengxiangeng@gmail.com (X.M.); shalaev@purdue.edu (V.M.S.)

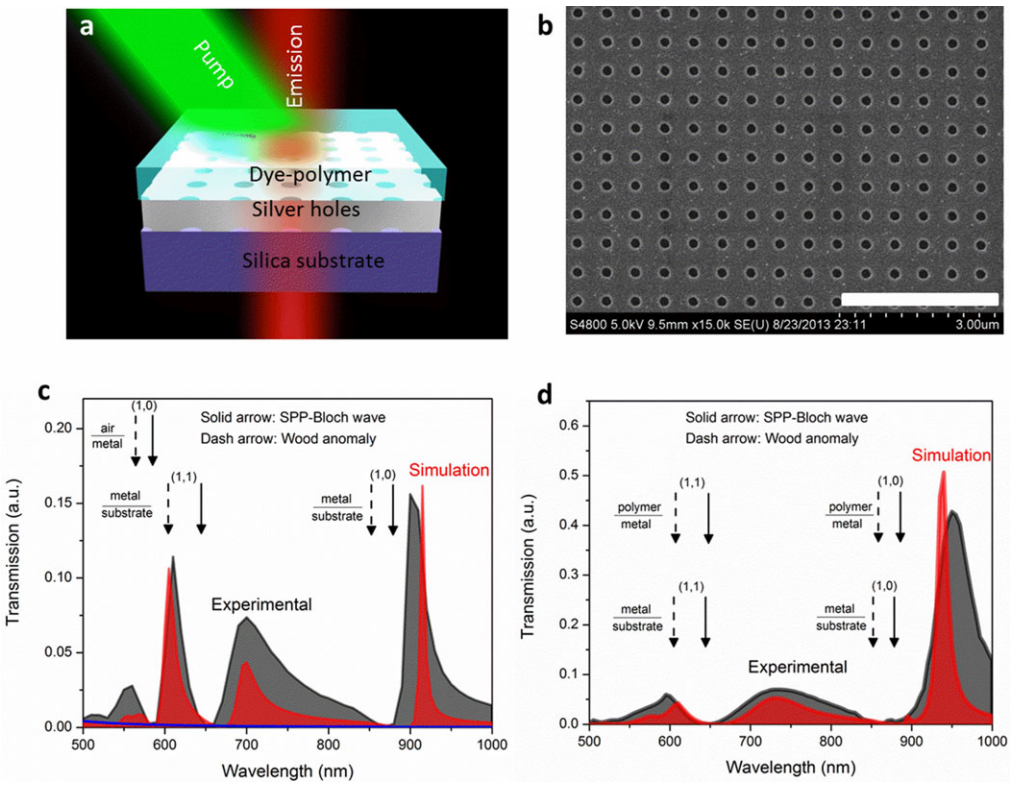

Figure 1 (a) Configuration of the spaser device. The system is composed of a periodic hole array covered by a thin layer of R101–PVA film. (b) SEM image of the hole array with d = 175 nm, t = 100 nm, and Λ = 565 nm. The white scale bar is 3 μm. (c, d) Transmission spectra of the holes exposed to air (c) and holes covered by PVA (d): experimental (black) and simulation (red) results. The transmission spectrum of the bare silver film (blue) is included in Fig. 1(c) for comparison. Markers indicate the central wavelength of the SPP–Bloch wave (solid markers) and the Wood anomaly (dashed markers) at the metal–air, metal–glass, and metal–PVA interfaces.

In this work, we demonstrate highly directional, room–temperature, and single–mode spaser emission in the red wavelength region. Our approach is to employ a metal film perforated with a periodic hole array, which support SPP–Bloch waves in the visible forming a plasmonic nanocavity, and an organic laser dye, which emits in the red portion of the spectrum, as the optical gain medium to amplify the SPP–Bloch wave. The resultant structure was optically pumped to study its lasing properties. When the pump power reaches a critical value, a single sharp peak suddenly appears at around $\lambda = 620$ nm with a spectral linewidth as narrow as $\sim$1.5 nm. The dependence of the peak emission intensity on the pump power shows a clear threshold behavior, suggesting the occurrence of spasing. In addition, the spaser emission propagates normal to the surface of the device with a rather small divergence angle. We prove that such spaser emission is not supported by an individual hole but is related to the SPP mode coupling by comparing with the emission properties of two systems: one with an aperiodic hole array and another with a periodic hole array which does not support SPP–Bloch waves at around the spasing frequency. In yet another control experiment, a hole array with identical dimensions perforated in a dielectric film was investigated but no lasing was achieved. This suggests the vital role of the plasmonic mode coupling in the occurrence of spasing.

2. Results and discussion

The configuration of the spaser device is depicted in Fig. 1(a), composed of a periodic sub–wavelength hole array patterned in a silver film on a transparent glass substrate, and covered with a thin layer of optical gain medium. Silver is chosen because of its low optical losses. The diameter, thickness, and the grating pitch of the holes are d = 175 nm, t = 100 nm, and Λ = 565 nm, respectively, as shown in Fig. 1(b). In contrast to the bare metal film that exhibits featureless transmission, the metal film perforated with the periodic hole array shows several intense transmission peaks in the visible and NIR wavelength regions. Such phenomenon, well–known as extraordinary optical transmittance, have been studied extensively [32–34]. The transmission spectrum of the holes exposed to air exhibits three major resonance peaks located at $\lambda = 610$ nm, 700 nm, and 900 nm, as shown in Fig. 1(c). The sharp resonance at $\lambda = 610$ nm has a narrow width of $\Delta\lambda \sim 13$ nm corresponding to a high quality factor of $Q = \lambda/\Delta\lambda \sim 47$. The other two resonances support Q factors of $\sim$ 26 and 33, respectively. It is noteworthy to mention that such sharp resonances are rather difficult to attain and are scarcely reported despite the fact that the properties of resonant plasmonic hole arrays have been extensively studied. As discussed below, such sharp resonances are vital for the observation of

spasing. Although the assignment of the transmission features observed in the sub–wavelength hole array perforated in a metal film still needs to be refined with more advanced methods, the transmission minima observed in Fig. 1(c) can be appropriately described with a simple SPP–Bloch wave model [32],

$$\mathrm{Re}\left[\frac{\omega}{c}\sqrt{\frac{\varepsilon_m\varepsilon_d}{\varepsilon_m+\varepsilon_d}}\right]=|k_0\sin\theta+iG_x+jG_y|, \quad (1)$$

where ω, c, and k_0 are the angular frequency, speed, and momentum of free–space light, ε_m and ε_d are the permittivities of the metal and dielectric, respectively; G_x and G_y denote additional momenta caused by the grating ($G_x = G_y = 2\pi/\Lambda$); integer index pairs (i, j) denote specific SPP modes. The transmission minima at $\lambda = 565$ nm, 645 nm, and 885 nm can be correlated with the $(1, 0)_{air}$, $(1, 1)_{glass}$, and $(1,0)_{glass}$ SPP–Bloch waves. The transmission maximum at $\lambda = 605$ nm is related to the Wood anomaly at $(1, 1)_{glass}$ that is described with the formula,

$$\frac{\omega}{c}\sqrt{\varepsilon_d}=|k_0\sin\theta+iG_x+jG_y|. \quad (2)$$

Figure 1(d) shows the transmission spectrum of the hole array covered by polyvinyl alcohol (PVA) which is used as the host medium of the laser dye (see below). Similar to the holes exposed to air, the transmission spectrum of the PVA–covered holes exhibits three major resonance peaks centered at $\lambda = 600$ nm, 730 nm, and 940 nm. As expected, the transmission minima corresponding to SPP–Bloch waves at the metal–glass interface appear at the same spectral positions as those with holes exposed to air, and the resonances at metal–air interface vanished in the PVA–covered holes. Moreover, the spectral positions of SPP–Bloch waves and Rayleigh anomalies at the metal–PVA interface resemble those at the metal–glass interface. This is understandable because the refractive index of PVA is rather close to that of the glass substrate (~1.5). We have performed calculations of the transmission spectrum using a finite–element method (Supporting information, Fig. S1). The calculations show excellent agreement with the experimental results (red curves in Figs. 1(c) & (d)). It is noteworthy to mention that a loss factor (α_l), which is defined by the geometry and fabrication quality of nanostructured silver, influences the permittivity of silver (Supporting information, Fig. S2). The best agreement between calculations and experiments (Figs. 1(c) &(d)) was attained by taking $\alpha_l = 1$, while for example calculations with $\alpha_l = 2$ give worse matching (Supporting information, Fig. S3).

The existence of SPP–Bloch waves indicates a strong SPP coupling, and suggests a route to achieve spasing with a high efficiency and low threshold. The $(1, 1)_{PVA}$ SPP–Bloch mode located at $\lambda = 645$ nm is of particular interest, since it provides a possibility to obtain SP amplification in the visible spectrum. Aiming at amplification of this mode, we chose an organic laser dye with a high quantum yield, Rhodamine 101 (R101), as the optical gain medium. R101 is a widely–studied laser dye for achieving lasing in the red–wavelength region [35]. To improve the chemical stability and prevent self–quenching of the dye molecules, we embedded R101 molecules inside PVA. For simplicity of the discussions hereafter, this optical gain composite is referred to as R101–PVA. A thin film of R101–PVA was deposited to cover the metal holes by spin–coating an aqueous solution containing PVA and R101. The film thickness is ~ 2.13 μm. The molecule density of R101 in PVA is approximately $\rho = 6 \times 10^{18}$ cm^{-3}. The optical absorption and fluorescence spectra of the R101–PVA thin film on the glass substrate are centered at 575 nm and 605 nm, respectively (Fig. 2, curves 1 & 2). The fluorescence spectrum of R101–PVA has a large overlap with the transmission spectrum of the PVA–covered holes (curve 3), indicating a significant coupling between the holes and optical gain medium.

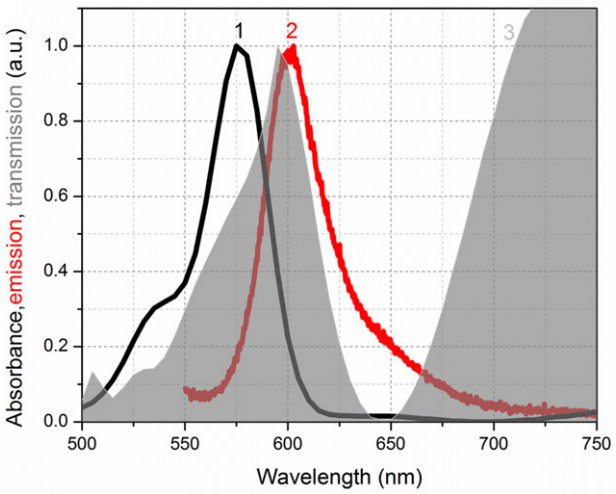

Figure 2 Optical properties of R101–PVA: the optical absorption (curve 1) and fluorescence spectra (curve 2) of the R101–PVA film. The transmission spectrum of the periodic hole array covered by PVA is included as well (curve 3) for comparison.

Figure 3(a) illustrates the excitation–detection scheme of lasing experiments. The sample was optically pumped by nanosecond laser pulses at $\lambda = 527$ nm. The emission signal was collected by an optical fiber and fed into a monochromator. Figure 3(b) shows the evolution of the emission spectrum with the pump power. At low pump power, the whole emission spectrum exhibits a rather weak signal with a high noise level. When the pump power increases, the emission signal changes slowly at first, and then a sharp peak appears at $\lambda = 620$ nm under a pump power of ~12 mW, accompanied by a rapid increase in the emission intensity. The emission is highly directional and normal to the surface of the sample. The spectral linewidth of this sharp peak is ~1.5 nm. This linewidth is limited by the spectral resolution of the current monochromator (~1 nm), and could be even narrower when detected by a monochromator with a higher resolution. In addition, a bright emission spot could be observed when the pump power reaches 12 mW. With a further increase of the pump power, the central wavelength of the narrow peak remains unchanged but the emission intensity increases rapidly. The dependence of the emission

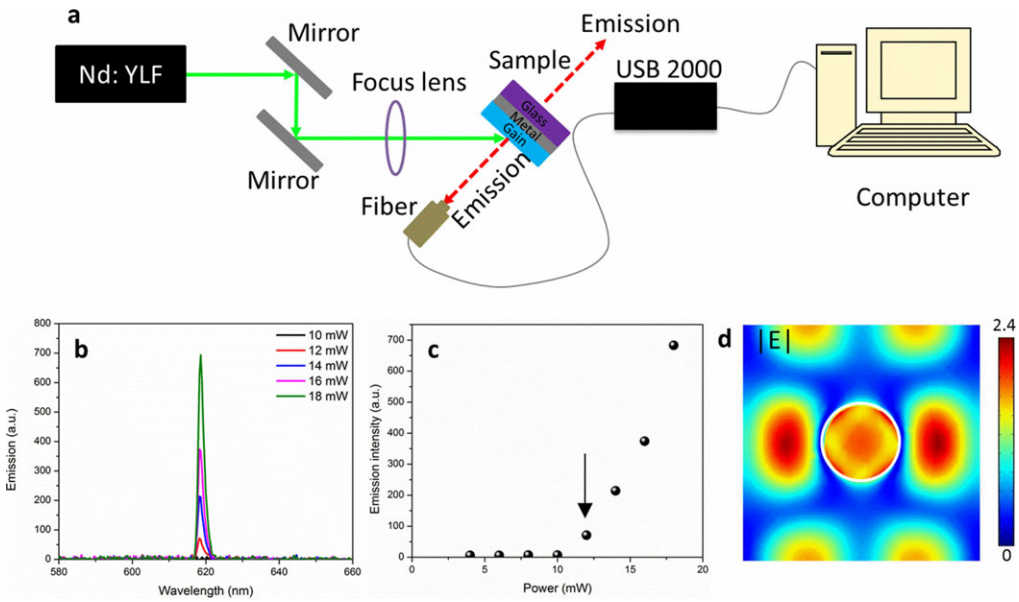

Figure 3 (a) Excitation–detection scheme. (b) Evolution of the emission spectrum with the pump power. The emission refers to the reflected signal herein. (c) Dependence of the peak emission intensity on the pump power. The arrow indicates the pump threshold. (d) Field distributions of a unit cell of the periodic hole array at $\lambda = 620$ nm, clearly showing the field coupling between holes.

peak intensity on the pump power shows a clear threshold behavior (Fig. 3(c)). The significant spectral narrowing and nonlinear increase of the emission signal with the pump power generally indicate the occurrence of spasing.

To prove the critical role of the SPP–Bloch wave in the occurrence of spasing, we have fabricated an aperiodic hole array with identical diameter, thickness, and number density of holes to those of periodic holes (Fig. 4(a)). It has been reported that aperiodic sub–wavelength apertures are capable of supporting distributed feedback and therefore can give rise to lasing [36, 37]. We note that such lasing has only been demonstrated in the terahertz region so far [37]. Similar to periodic holes, the aperiodic hole array shows obvious plasmonic resonances in the visible and NIR regions, as shown in Fig. 4(b). However, these resonances are not as sharp, and exhibit a lower transmission magnitude when compared to the periodic holes. We fabricated an active system by depositing a R101-PVA thin film on the aperiodic holes, and examined the corresponding emission properties upon optical pumping with nanosecond pulses as mentioned above. Figure 4(c) describes the evolution of the emission spectrum with the pump power. We only observed a weak signal with a broad emission linewidth. This is far from the occurrence of spasing. In addition, the peak emission intensity increases rather slowly and almost linearly with the pump power, again suggesting no sign of spasing action. Moreover, we designed a periodic hole array in a silver film which shows a broad transmission spectrum with the resonance of an individual hole at around $\lambda = 600$ nm. This was made by reducing the grating pitch to $\Lambda = 300$ nm. The resonance of the individual holes is intense but the effect of hole–to–hole coupling is not obvious such that no SPP waves are excited at this wavelength. As a result, this structure does not show spasing (Supporting information, Fig. S4).

The absence of spasing in the supplementary systems fabricated with aperiodic holes and periodic holes with a reduced grating pitch strongly suggest that the spasing observed in the original system is associated with the plasmonic mode coupling between holes, instead of the plasmonic resonance in an individual hole. Thus, we suggest that the optical feedback for spasing is supplied by the SPP–Bloch wave. Although the SPP–Bloch wave appears in both the metal–glass and metal–polymer interfaces with almost identical spectral positions (Fig. 1(d)), the SPP–Bloch wave at metal–polymer interface should predominantly contribute to the occurrence of spasing since the optical gain medium is accumulated on this interface. It is important to mention that the occurrence of spasing is not exactly at the central wavelength of the $(1, 1)_{PVA}$ SPP–Bloch wave ($\lambda = 645$ nm), but at a somewhat shorter wavelength of $\lambda = 620$ nm. The blue–shift of the spasing wavelength relative to the $(1, 1)_{PVA}$ SPP–Bloch mode is because the fluorescence peak of R101–PVA is located at a shorter wavelength ($\lambda = 605$ nm, Fig. 2), where the dye molecules provide a higher level of optical gain. To understand the mechanism responsible for spasing, we performed numerical simulations to look into the electric field distributions. The simulation was conducted on a single unit cell of the periodic hole array for a passive structure composed of the array covered by PVA. Here we provide the electric field distributions at the metal–PVA interface where most of optical gain media are located to enable spasing. As shown in Fig. 3(d), although the spasing is slightly shifted from the SPP–Bloch central wavelength, an obvious mode coupling exists at $\lambda = 620$ nm, which is quite similar to that

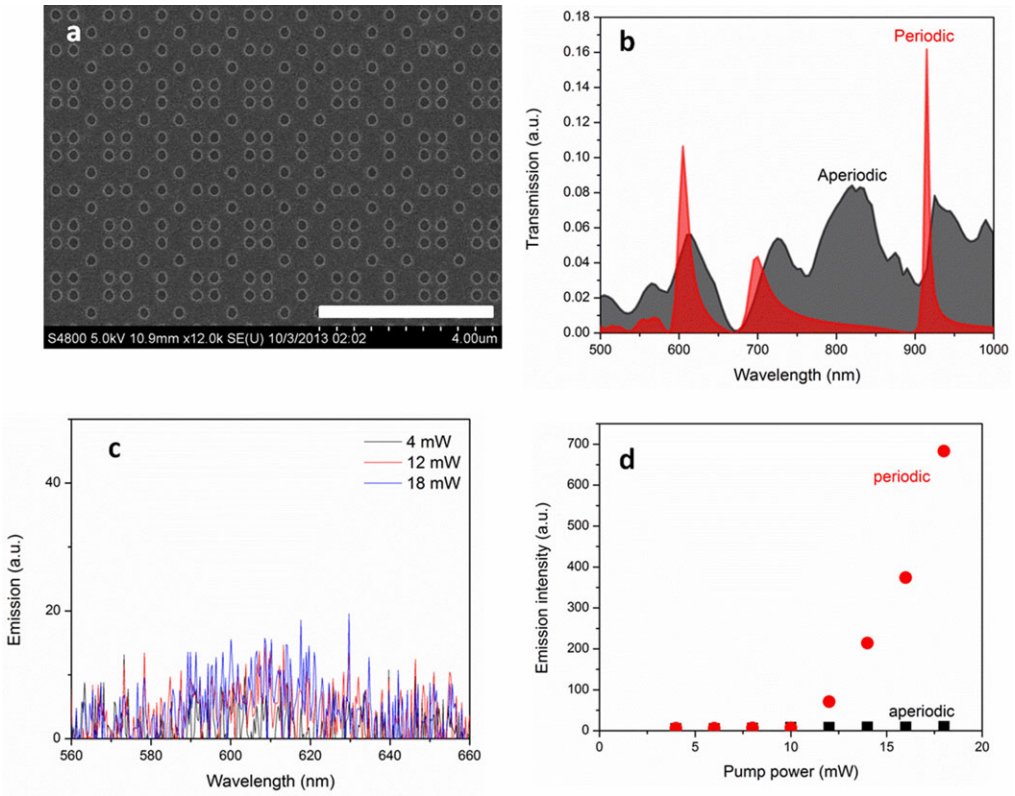

Figure 4 (a) SEM image of aperiodic holes. The white scale bar is 4 μm. (b) Comparison of the transmission spectrum between aperiodic (black) and periodic holes (red) when they are exposed to air. (c) Evolution of the emission spectrum with the pump power for the sample based on aperiodic holes. (d) Dependence of the peak emission intensity on the pump power for the samples based on aperiodic (black) and periodic holes (red).

at the SPP–Bloch central wavelength, and extends over a broad wavelength region (Supporting information, Fig. S5). Therefore, such mode coupling is capable of providing an intense optical feedback for spasing.

We have examined the spatial distribution of the spasing emission by scanning an optical fiber (mounted in a three–dimensional optical translation stage) across the spaser emission spot and recording the corresponding emission signal. The results are plotted in Figs. 5(a) and (b), showing that the spasing emission has a small divergence angle on the scale of $1 \sim 3°$. This feature resembles what has been observed in a similar plasmonic nanolaser based on periodic metal nanodisks and operating in the NIR wavelength region [28]. Fig. 5(c) shows the spectra of the reflected and transmitted emission signals. These two emission spectra are almost identical to each other in terms of spectral profile and resonant wavelength. It is natural to have such a phenomenon because the periodic metal holes exhibit enhanced optical transmission around the spasing wavelength. This is a unique feature in comparison to the plasmonic nanolaser based on periodic metal disks of Ref. 28.

As an additional control experiment, an optical system with the same–dimensional periodic hole array perforated in an alumina film was fabricated, and its ability to achieve lasing was examined. This all–dielectric system does not show any lasing (Supporting information, Fig. S6), indicating the vital role of the plasmonic resonance in the occurrence of spasing observed above. It should be noted that as previously shown, a bare metal thin film was able to initiate lasing actions when the surface roughness of the metal film was engineered to some extent [38]. However, the mechanism for this lasing is quite different. It results from light scattering caused by the surface roughness which fosters optical feedback for lasing. Such lasing is classified as random lasing. We have examined the possibility to obtain lasing in a sample based on a bare 100 nm–thick silver thin film, and did not find any lasing even at rather high pump power (Supporting information, Fig. S7). The absence of lasing is presumably due to the fact that the surface of our metal film here is rather smooth and unable to provide sufficient light scattering for optical feedback, illustrating the importance of the holey structure in our case.

It is important to mention that the hole array we fabricated has a rather smooth surface and supports intense plasmonic resonances. This high–quality pattern is a necessity for the observation of spasing. To check this we have fabricated a periodic hole array with poor quality, and the resultant structure did not show any spasing (Supporting information, Fig. S8).

It is also noteworthy to mention that the plasmonic cavity of our work is fabricated prior to the deposition of the optical gain media, which is distinct from a recent report

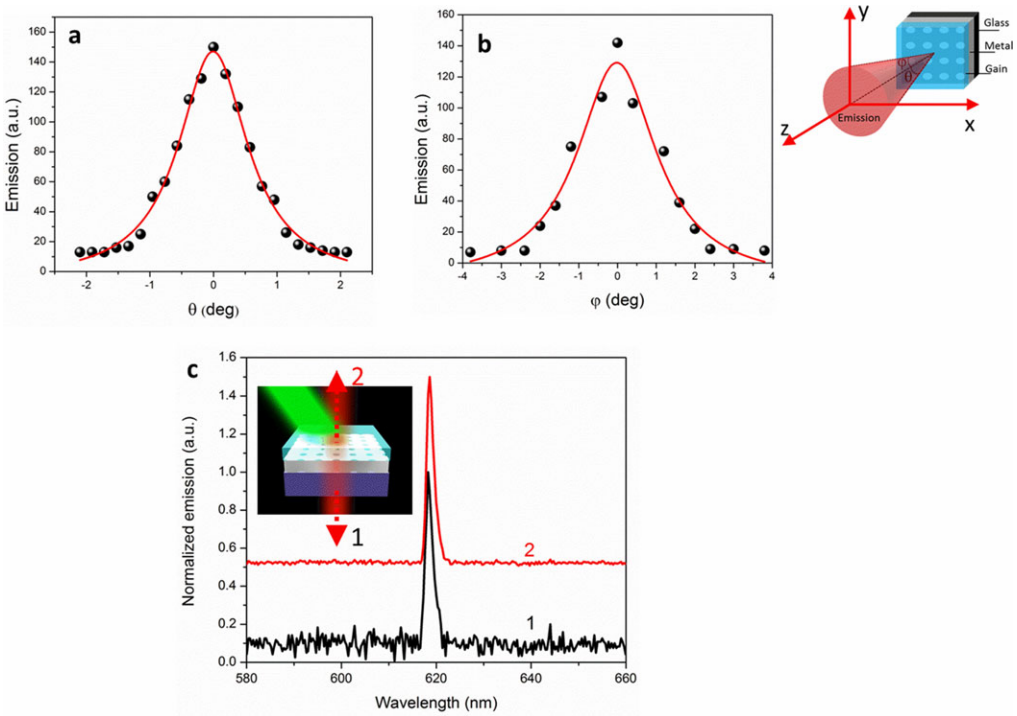

Figure 5 (a, b) Spatial distribution of the lasing emission observed in periodic holes along horizontal (a) and vertical (b) directions. The insert shows the schematic of the divergence angles θ and ϕ. (c) Emission spectra of reflected (curve 1) and transmitted (curve 2) lasing signals.

where spasing is achieved in a metal hole array which acts as plasmonic cavities [27]. This configuration ensures that the chemical composition of the optical gain media is not influenced by fabrication of plasmonic nanostructures, enabling a high effective optical gain. Moreover, the use of organic dyes allows easy control of the effective optical gain by changing the doping concentration of dyes. These important features are vital to the achievement of room–temperature spasing in the visible.

3. Conclusion

To conclude, we have fabricated a high–quality periodic hole array perforated in a silver film that exhibits intense plasmonic resonances in the visible and NIR wavelength regions. A spaser system was developed by covering such a hole array with a dye–polymer film as the optical gain medium, and the resultant device exhibits spasing emission upon optical pumping with nanosecond pulses. The spasing occurs in the red–wavelength region with highly-directional emission, and operates at room temperature with a single mode. We excluded the role of plasmonic resonance from an individual hole as the basis for spasing due to the absence of spasing emission in control systems based on aperiodic holes and periodic holes that do not support the SPP–Bloch wave at around the spasing wavelength. We suggest that the optical feedback for spasing was provided by the SPP–Bloch wave existing at the metal–polymer interface. We expect this work demonstrating efficient directional radiation in the visible from plasmonic nanolaser sources will further advance the fundamentals of nanolasers.

4. Experimental section

4.1. Fabrication of periodic hole array in metal film

A large array of holes was patterned on an ITO–coated glass substrate using electron beam lithography. Patterns were defined on the negative tone resist hydrogen silsesquioxane (HSQ). The process began by spin–coating PMMA–A4 on an ITO–coated glass substrate, followed by soft–baking. HSQ was then spin–coated on the PMMA film, which is soft–baked again. A 500 μm $\times$ 500 μm dimension of 565 nm–diameter holes was patterned by exposing the resist, and developing the resist in 25% tetramethylammonium hydroxide (TMAH) at room temperature. The lithographically defined pattern was transferred into the PMMA layer by dry etching in an inductively coupled plasma (ICP) RIE system using O_2. A 100 nm–thick Ag layer was electron–beam–evaporated onto the patterned substrate. The sample was lifted–off by acetone to remove PMMA together with HSQ.

4.2. Optical and structural characterization

The optical absorption spectrum of R101–PVA thin film was measured in a commercial UV–visible–near infrared

spectrometer (Lambda 950). The optical transmission spectrum of the metal holes was measured by an ellipsometer (W–VASE, J. A. Woollam Co., Inc.). The fluorescence spectrum was recorded by exciting the sample at $\lambda = 527$ nm and collecting the emission by an optical fiber to a monochromator. A field–emission scanning electron microscope (Hitachi S4800) was used to record the SEM image of holes.

4.3. Lasing experiments

In lasing experiments, the sample was mounted in a three–dimensional optical translation stage so that the position of the sample could be finely adjusted. The pumping source was a nanosecond Nd: YLF laser (operation wavelength: 527 nm; pulse duration: 200 ns, and repetition rate: 1 Hz). The pump beam was incident on the sample surface through a focusing lens ($f = 20$ nm) to form a 0.9 mm–diameter pump spot. The incident angle was set as 30° for all experiments, unless specified elsewhere. An optical fiber was placed at a distance of $L = 6$ cm away from the sample surface to collect the emission signal. A monochromator (Ocean Optics USB 2000, resolution: 1 nm) was used to record the data. To analyze the spatial distribution of the lasing emission, the optical fiber was scanned horizontally and vertically with a step of 0.1 mm and the corresponding emission signal was recorded. The central position ($x = 0$, $y = 0$) was where we obtained the most intense emission signal. The values of θ and ϕ were calculated by $\tan\theta = \Delta x/L$ and $\tan\phi = \Delta y/L$, where Δx and Δy are the distances from the central position along horizontal and vertical directions.

Acknowledgements. The authors acknowledge financial support by Office of Naval Research Grant (MURI N00014-13-0649), Air Force Office of Scientific Research Grant (FA9550-10-1-0264), National Science Foundation Grant (DMR-1120923), and NSF "Meta–PREM" grant (1205457). The authors thank Naresh K. Emani for assistance in fabrication of Fibonacci holes.

Supporting Information: for this article is available free of charge under http://dx.doi.org/10.1002/lpor.201400056

Received: 11 March 2014, **Revised:** 9 May 2014,
Accepted: 14 May 2014

Published online: 18 June 2014

Key words: Plasmonics, spaser, subwavelength hole array, directional emission.

References

[1] D. J. Bergman and M. I. Stockman, Phys. Rev. Lett. **90**, 027402 (2003).
[2] J. Seidel, S. Grafström, and L. Eng, Phys. Rev. Lett. **94**, 177401 (2005).
[3] M. A. Noginov, G. Zhu, M. Mayy, B. A. Ritzo, N. Noginova, and V. A. Podolskiy, Phys. Rev. Lett. **101**, 226806 (2008).
[4] S. A. Maier, Opt. Comm. **258**, 295–299 (2006).
[5] P. Berini and I. De Leon, Nat. Photon. **6**, 16–24 (2012).
[6] S. Wuestner, A. Pusch, K. L. Tsakmakidis, J. M. Hamm, and O. Hess, Phys. Rev. Lett. **105**, 127401 (2010).
[7] J. A. Gordon and R. W. Ziokowski, Opt. Express **15**, 2622–2653 (2007).
[8] T. Okamoto, J. Simonen, and S. Kawata, Phys. Rev. **77**, 115425B (2008).
[9] M. Wegner, J. L. García–Pomar, C. M. Soukoulis, N. Meinzer, M. Ruther, and S. Linden, Opt. Express **16**, 19785–19798 (2008).
[10] N. I. Zheludev, S. L. Prosvirnin, N. Papasimakis, and V. A. Fedotov, Nat. Photon. **2**, 351–354 (2008).
[11] M. I. Stockman, J. Opt. **12**, 024004 (2010).
[12] X. Meng, U. Guler, A. V. Kildishev, K. Fujita, K. Tanaka, and V. M. Shalaev, Sci. Rep. **3**, 1241 (2013).
[13] M. T. Hill, Y. Oei, B. Smalbrugge, Y. Zhu, T. de Vries, P. J. van Veldhoven, F. W. M. van Otten, T. J. Eijkemans, J. P. Turkiewicz, H. de Waardt, E. J. Geluk, S. Kwon, Y. Lee, R. Nötzel, and M. K. Smit, Nat. Photon. **1**, 589–594 (2007).
[14] M. A. Noginov, G. Zhu, A. M. Belgrave, R. Bakker, V. M. Shalaev, E. E. Narimanov, S. Stout, E. Herz, T. Suteewong, and U. Wiesner, Nature **460**, 1110–1113 (2009).
[15] R. F. Oulton, V. J. Sorger, T. Zentgraf, R. Ma, C. Gladden, L. Dai, G. Bartal, and X. Zhang, Nature **461**, 629–632 (2009).
[16] R. Ma, R. F. Oulton, V. J. Sorger, G. Bartal, and X. Zhang, Nat. Mater. **10**, 110–113 (2011).
[17] C. Y. Wu, C. T. Kuo, C. Y. Wang, C. L. He, M. H. Lin, H. Ahn, and S. Gwo, Nano Lett. **11**, 4256–4260 (2011).
[18] Y. J. Lu, J. Kim, H. Y. Chen, C. Wu, N. Dabidian, C. E. Sanders, C. Y. Wang, M. Y. Lu, B. H. Li, X. Qiu, W. H. Chang, L. J. Chen, G. Shvets, C. K. Shih, and S. Gwo, Science **337**, 450–453 (2012).
[19] R. M. Ma, X. Yin, R. F. Oulton, V. J. Sorger, and X. Zhang, Nano Lett. **12**, 5396–5402 (2012).
[20] J. K. Kitur, V. A. Podolskiy, and M. A. Noginov, Phys. Rev. Lett. **106**, 183903 (2011).
[21] X. Meng, A. V. Kildishev, K. Fujita, K. Tanaka, and V. M. Shalaev, Nano Lett. **13**, 4106–4112 (2013).
[22] K. Ding, Z. C. Liu, L. J. Yin, M. T. Hill, M. J. H. Marell, P. J. van Veldhoven, R. Noetzel, and C. Ning, Phys. Rev. B **85**, 041301 (2012).
[23] M. P. Nezhad, A. Simic, O. Bondarenko, B. Slutsky, A. Mizrahi, L. Feng, V. Lomakin, and Y. Fainman, Nat. Photon. **4**, 395–3999 (2010).
[24] M. Khajavikhan, A. Simic, J. H. Lee, B. Slutsky, A. Mizrahi, V. Lomakin, and Y. Fainman, Nature **482**, 204–207 (2012).
[25] M. C. Gather, K. Meerholz, N. Danz, and K. Leosseon, Nat. Photon. **4**, 457–461 (2010).
[26] I. De Leon and P. Berini, Nat. Photon. **4**, 382–387 (2010).
[27] A. A. Zyablovsky, A. V. Dorofeenko, A. P. Vinogradov, E. S. Andrianov, A. A. Pukhov, and A. A. Lisyansky, AIP Conf. Proc. **1475**, 185–187 (2012).
[28] A. V. Dorofeenko, A. A. Zyablovsky, A. P. Vinogradov, E. S. Andrianov, A. A. Pukhov, and A. A. Lisyansky, Opt. Express **21**, 14539–14547 (2013).
[29] F. van Beijnum, P. J. van Veldhoven, E. J. Geluk, M. J. A. de Dood, G. W. 't Hooft, and M. P. van Exter, Phys. Rev. Lett. **110**, 206802 (2013).
[30] W. Zhou, M. Dridi, J. Y. Suh, C. H. Kim, D. T. Co, M. R. Wasielewski, G. C. Schatz, and T. W. Odom, Nat. Nanotech. **8**, 506–511 (2013).

[31] R. Marani, A. D'Orazio, V. Petruzzelli, S. G. Rodrigo, L. Martin-Moreno, F. J. García-Vidal, and J. Bravo-Abad, New J. Phys. **14**, 013020 (2012).
[32] T. W. Ebbesen, H. J. Lezec, H. F. Ghaemi, T. Thio, and P. A. Wolff, Nature **391**, 667–669 (1998).
[33] H. F. Ghaemi, T. Thio, D. E. Grupp, T. W. Ebbesen, and H. J. Lezec, Phys. Rev. B **58**, 6779–6782 (1998).
[34] S. H. Chang, S. K. Gray, and G. C. Schatz, Opt. Express **13**, 3150–3165 (2005).
[35] X. Meng, K. Fujita, Y. Moriguchi, Y. Zong, and K. Tanaka, Adv. Opt. Mater. **1**, 573–580 (2013).
[36] T. Matsui, A. Agrawal, A. Nahata, and Z. V. Vardeny, Nature **446**, 517–521 (2007).
[37] L. Mahler, A. Tredicucci, F. Beltram, C. Walther, J. Faist, H. E. Beere, D. A. Ritchie, and D. S. Wiersma, Nat. Photon. **4**, 165–169 (2010).
[38] M. Kawasaki and S. Mine, J. Phys. Chem. B **110**, 15052–15054 (2006).